

# Decorrelation of sequences of medical CT images based on the hierarchical adaptive KLT

Roumen Kountchev, Peter Ivanov

Technical University of Sofia, Department of Radio Communications and Video Technologies,  
Boul. Kl. Ohridsky 8, Sofia 1000, Bulgaria

rkountch@tu-sofia.bg; peter.n.ivanov@gmail.com

**Abstract.** In this work is presented one new approach for processing of sequences of medical CT images, called Hierarchical Adaptive Karhunen-Loeve Transform (HAKLT). The aim is to achieve high decorrelation for each group of 9 consecutive CT images, obtained from the original larger sequence. In result, the main part of the energy of all images in one group is concentrated in a relatively small number of eigen images. This result could be obtained using the well-known Karhunen-Loeve Transform (KLT) with transformation matrix of size  $9 \times 9$ . However, for the implementation of the 2-levels HAKLT in each level are used 3 transform matrices of size  $3 \times 3$ , in result of which the computational complexity of the new algorithm is reduced in average 2 times, when compared to that of KLT with  $9 \times 9$  matrix. One more advantage is that the algorithm permits parallel processing for each group of 3 images in every hierarchical level. In this work are also included the results of the algorithm modeling for sequences of real CT images, which confirm its ability to carry out efficient decorrelation. The HAKLT algorithm could be farther used as a basis for the creation of algorithms for efficient compression of sequences of CT images and for features space minimization in the regions of interest, which contain various classes of searched objects.

**Keywords:** Decorrelation of medical CT image sequences, Hierarchical Adaptive Karhunen-Loeve Transform (HAKLT), Group of Medical Images.

## 1 Introduction

In the last years, large number of new technologies and systems for digital processing of medical images had been created [1, 2, 3], such as: the standard Digital Imaging and Communication in Medicine (DICOM) [4] used for storage, transfer and visualization of images, obtained from computer tomographic systems, MRI and ultrasound scanners; Picture Archiving and Communication System (PACS); systems for digital radiography, teleradiology, etc. Medical images could be still or moving, such as Magnetic Resonance Image (MRI), Nuclear Magnetic Resonance Image (NMRI), Magnetic Resonance Tomography Image (MRTI), etc. Moving images are represented by sequences of still images, obtained in consecutive time moments, or

spatial positions of the Computer Tomography (CT) scanner. Because of the large volume of the visual medical information, various algorithms are used for its compression. For still MRI are usually used algorithms based on the DCT, wavelet decomposition for prediction or zero-tree/block coding [5, 6, 7], etc. For compression of CT images sequences are used: interframe decorrelation based on hierarchical interpolation (HINT) [8, 9], spatial active appearance model [10], JPEG-LS and JPEG2000 with interframe motion compensated prediction [11, 12] and distributed representation of image sets based on Slepian-Wolf coding [13].

One of the most efficient methods for decorrelation and compression of groups of images is based on the KLT, also known as transform of Hotelling, or Principal Component Analysis (PCA) [14] - [23]. For its implementation the pixels with the same spatial position in a group of  $N$  images compose the corresponding  $N$ -dimensional vector. The basic difficulty of the KLT implementation is related to the large size of the covariance matrix. For the calculation of its eigenvectors is necessary to calculate the roots of a polynomial of  $n^{\text{th}}$  degree (characteristic equation) and to solve a linear system of  $N$  equations. For large values of  $N$ , the computational complexity of the algorithm for calculation of the transform matrix is significantly increased.

One of the possible approaches for reduction of the computational complexity of KLT for  $N$ -dimensional group of medical images is based on the "Hierarchical Adaptive KLT" (HAKLT), offered in this work. Unlike the famous hierarchical KLT (HKLT) [18], this transform is not related to the image sub-blocks, but to the whole image from one group. For this, the HAKLT is implemented through dividing the image sequence into sub-groups of 3 images each, on which is applied Adaptive KLT (AKLT), of size  $3 \times 3$ . This transform is performed using equations, which are not based on iterative calculations, and as a result, they have lower computational complexity. To decorrelate the whole group of medical images is necessary to use AKLT of size  $3 \times 3$ , which to be applied in several consecutive stages (hierarchical levels), with rearranging of the obtained intermediate eigen images after each stage. In result is obtained a decorrelated group of 9 eigen medical images.

The paper comprises the following: the principle for decorrelation of CT images group through HAKLT, the calculation of eigen images through AKLT with  $3 \times 3$  matrix, experimental results, evaluation of the computational complexity and conclusions.

## **2 Principle for Decorrelation of a Group of CT Images Through Hierarchical AKLT**

The sequence of medical images is divided into Groups of 9 Images (GMI), for which is supposed that they are highly correlated. On the other hand, each GMI is further divided into 3 sub-groups.

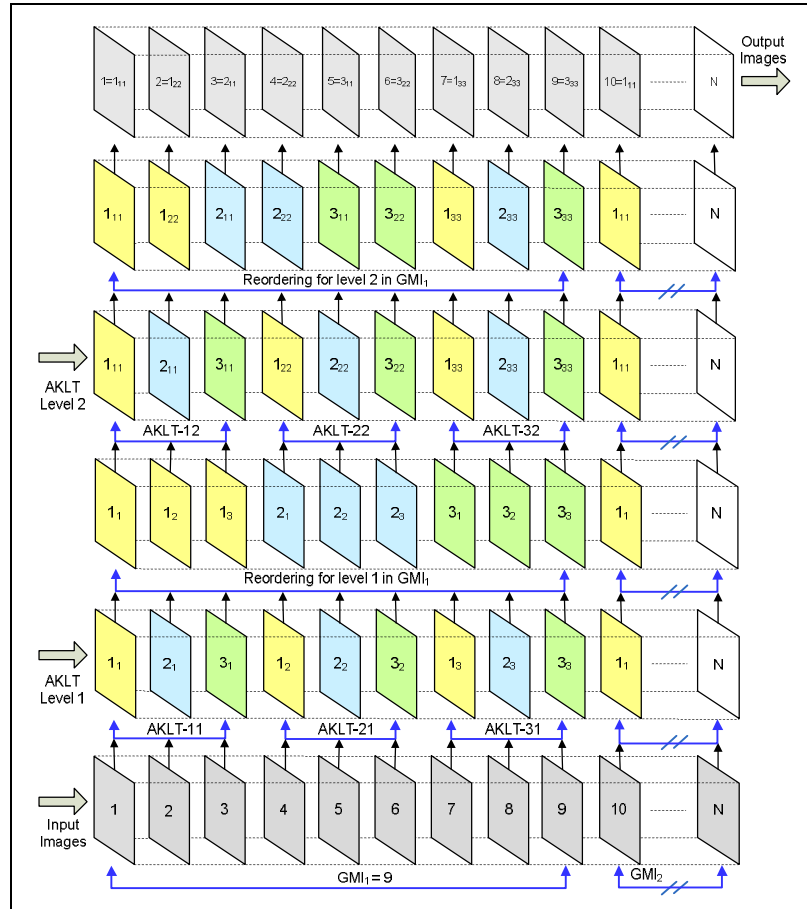


**Fig. 1.** Algorithm for 2-levels Hierarchical Adaptive KLT for Group of 9 Medical Images

The algorithm for 2-levels HAKLT for one GMI is shown on Fig. 1. As it is easily seen there, on each sub-group of 3 images from the first hierarchical level of HAKLT is applied AKLT with matrix of size  $3 \times 3$ . In result are obtained 3 eigen images, colored in yellow, blue and green correspondingly. After that, the eigen images are rearranged so that the first sub-group of 3 eigen images to comprise the first images from each group, the second group of 3 eigen images – the second images from each group, etc. For each GMI of 9 intermediate eigen images in the first hierarchical level is applied in similar way the next AKLT, with a  $3 \times 3$  matrix, on each sub-group of 3 eigen values. In result are obtained 3 new eigen images (i.e. the eigen images of the group of 3 intermediate eigen images), colored in yellow, blue, and green correspondingly in the second hierarchical level. Then the eigen images are rearranged again so, that the first group of 3 eigen images to contain the first images

from each group before the rearrangement; the second group of 3 eigen images - the second image before the rearrangement, etc. At the end of the processing is obtained a decorrelated sequence of eigen images, using which and through inverse HAKLT could be restored the original sequence.

### 3 Calculation of Eigen Images Through AKLT with 3×3 Matrix

For the calculation of eigen images through AKLT with 3×3 matrix for GMI sub-group is used the approach, given in [24] for the representation of the 3D color vector in the KLT space. From each sub-group with 3 medical images of  $S$  pixels each, shown on Fig. 2, are calculated the vectors  $\vec{C}_s = [C_{1s}, C_{2s}, C_{3s}]^t$  for  $s=1, 2, \dots, S$  (on the figure are shown the vectors for the first 4 pixels only, resp.  $\vec{C}_1 = [C_{11}, C_{21}, C_{31}]^t, \vec{C}_2 = [C_{12}, C_{22}, C_{32}]^t, \vec{C}_3 = [C_{13}, C_{23}, C_{33}]^t, \vec{C}_4 = [C_{14}, C_{24}, C_{34}]^t$ ). Each vector is then transformed into corresponding vectors  $\vec{L}_s = [L_{1s}, L_{2s}, L_{3s}]^t$  through APCA with the matrix  $[\Phi]$  of size 3×3. Its elements  $\Phi_{ij}$  are defined below:

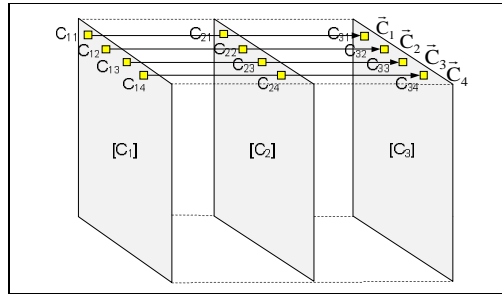


Fig. 2. Sub-group of 3 images from the GMI

❖ The covariance matrix  $[K_C]$  of size 3×3 for vectors  $\vec{C}_s$  is calculated:

$$[K_C] = \left[ \frac{1}{S} \sum_{s=1}^S \vec{C}_s \vec{C}_s^t \right] - \bar{m}_c \bar{m}_c^t = \begin{bmatrix} k_{11} & k_{12} & k_{13} \\ k_{21} & k_{22} & k_{23} \\ k_{31} & k_{32} & k_{33} \end{bmatrix}, \quad (1)$$

where  $\bar{m}_c = [\bar{C}_1, \bar{C}_2, \bar{C}_3]^t$  is the mean vector. Here  $\bar{x} = E(x_s) = \frac{1}{S} \sum_{s=1}^S x_s$ ;  $E(\cdot)$  – operator for calculation of the mean value of  $x_s$  for  $s = 1, 2, \dots, S$ .

❖ The elements of the mean vector  $\bar{m}_c$  and of the matrix  $[K_C]$  are defined in accordance with the relations:

$$\bar{C}_1 = E(C_{1s}), \quad \bar{C}_2 = E(C_{2s}), \quad \bar{C}_3 = E(C_{3s}), \quad (2)$$

$$k_{11}=k_1=E(C_{1s}^2)-(\bar{C}_1)^2, k_{22}=k_2=E(C_{2s}^2)-(\bar{C}_2)^2, k_{33}=k_3=E(C_{3s}^2)-(\bar{C}_3)^2, \quad (3)$$

$$k_{12}=k_{21}=k_4=E(C_{1s}C_{2s})-(\bar{C}_1)(\bar{C}_2), k_{23}=k_{32}=k_6=E(C_{2s}C_{3s})-(\bar{C}_2)(\bar{C}_3), \quad (4)$$

$$k_{13}=k_{31}=k_5=E(C_{1s}C_{3s})-(\bar{C}_1)(\bar{C}_3). \quad (5)$$

❖ The eigen values  $\lambda_1, \lambda_2, \lambda_3$  of the matrix  $[K_C]$  are defined in accordance to the solution of the characteristic equation:

$$\det|k_{ij}-\lambda\delta_{ij}|=\lambda^3+a\lambda^2+b\lambda+c=0, \quad (6)$$

$$\text{where: } \delta_{ij}=\begin{cases} 1, & i=j, \\ 0, & i\neq j. \end{cases}$$

$$\begin{aligned} a &= -(k_1+k_2+k_3), \quad b = k_1k_2+k_1k_3+k_2k_3-(k_4^2+k_5^2+k_6^2), \\ c &= k_1k_6^2+k_2k_5^2+k_3k_4^2-(k_1k_2k_3+2k_4k_5k_6), \end{aligned} \quad (7)$$

Since the matrix  $[K_C]$  is symmetric, its eigen values are real numbers. For their calculation could be used the equations of Cardano for “casus irreducibilis” (i.e., the so-called “trigonometric solution”):

$$\lambda_1=2\sqrt{\frac{|p|}{3}}\cos\left(\frac{\varphi}{3}\right)-\frac{a}{3}; \lambda_2=-2\sqrt{\frac{|p|}{3}}\cos\left(\frac{\varphi+\pi}{3}\right)-\frac{a}{3}; \quad (8)$$

$$\lambda_3=-2\sqrt{\frac{|p|}{3}}\cos\left(\frac{\varphi-\pi}{3}\right)-\frac{a}{3} \quad \text{for } \lambda_1 \geq \lambda_2 \geq \lambda_3 \geq 0,$$

$$q=2(a/3)^3-(ab)/3+c, \quad p=-(a^2/3)+b < 0, \quad (9)$$

$$\varphi = \arccos\left[-q/2/\sqrt{(|p|/3)^3}\right],$$

❖ The eigen vectors  $\bar{\Phi}_1, \bar{\Phi}_2, \bar{\Phi}_3$  of the covariance matrix  $[K_C]$  are the solution of the system of equations below:

$$[K_C]\bar{\Phi}_m = \lambda_m\bar{\Phi}_m \quad \text{and} \quad |\bar{\Phi}_m|^2 = \sum_{i=1}^3 \Phi_{mi}^2 = 1, \quad \text{for } m=1,2,3. \quad (10)$$

Eq. 10 follows from the condition for orthogonality and normalization of all 3 eigenvectors:

$$\bar{\Phi}_s' \bar{\Phi}_k = \sum_{i=1}^3 \Phi_{is} \Phi_{ik} = \begin{cases} 1 & \text{for } s=k; \\ 0 & \text{for } s\neq k. \end{cases} \quad \text{for } s, k = 1,2,3. \quad (11)$$

The solution of the system of equations (10) is used to calculate components of  $m^{\text{th}}$  eigenvector  $\bar{\Phi}_m = [\Phi_{1m}, \Phi_{2m}, \Phi_{3m}]^t$ , which corresponds to the eigen value  $\lambda_m$ :

$$\Phi_{1m} = A_m/P_m; \Phi_{2m} = B_m/P_m; \Phi_{3m} = D_m/P_m, \text{ for } m = 1, 2, 3; \quad (12)$$

$$A_m = (k_3 - \lambda_m) [k_5(k_2 - \lambda_m) - k_4 k_6], B_m = (k_3 - \lambda_m) [k_6(k_1 - \lambda_m) - k_4 k_5], \quad (13)$$

$$D_m = k_6 [2k_4 k_5 - k_6(k_1 - \lambda_m)] - k_5^2(k_2 - \lambda_m), P_m = \sqrt{A_m^2 + B_m^2 + D_m^2} \neq 0. \quad (14)$$

The KLT matrix  $[\Phi]$  comprises the eigenvectors  $\bar{\Phi}_m = [\Phi_{1m}, \Phi_{2m}, \Phi_{3m}]^t$ :

$$[\Phi] = \begin{bmatrix} \bar{\Phi}_1^t \\ \bar{\Phi}_2^t \\ \bar{\Phi}_3^t \end{bmatrix} = \begin{bmatrix} \Phi_{11} & \Phi_{21} & \Phi_{31} \\ \Phi_{12} & \Phi_{22} & \Phi_{32} \\ \Phi_{13} & \Phi_{23} & \Phi_{33} \end{bmatrix}, \text{ for } m = 1, 2, 3. \quad (15)$$

The direct AKLT for vectors  $\bar{C}_s = [C_{1s}, C_{2s}, C_{3s}]^t$ , from which are obtained vectors  $\bar{L}_s = [L_{1s}, L_{2s}, L_{3s}]^t$ , is:

$$\begin{bmatrix} L_{1s} \\ L_{2s} \\ L_{3s} \end{bmatrix} = \begin{bmatrix} \Phi_{11} & \Phi_{21} & \Phi_{31} \\ \Phi_{12} & \Phi_{22} & \Phi_{32} \\ \Phi_{13} & \Phi_{23} & \Phi_{33} \end{bmatrix} \begin{bmatrix} (C_{1s} - \bar{C}_1) \\ (C_{2s} - \bar{C}_2) \\ (C_{3s} - \bar{C}_3) \end{bmatrix} \text{ for } s = 1, 2, \dots, S. \quad (16)$$

The components of vectors  $\bar{L}_s = [L_{1s}, L_{2s}, L_{3s}]^t$  could be processed in various way (such as for example: orthogonal transforms, quantization, decimation and interpolation, etc.). In result are obtained the corresponding vectors  $\bar{L}_s^q = \psi(\bar{L}_s) = [\psi_1(L_{1s}), \psi_2(L_{2s}), \psi_3(L_{3s})]^t$  with components  $L_{1s}^q = \psi_1(L_{1s})$ ,  $L_{2s}^q = \psi_2(L_{2s})$ ,  $L_{3s}^q = \psi_3(L_{3s})$ , where  $\psi_1(\cdot), \psi_2(\cdot), \psi_3(\cdot)$  are the functions of the used transform. For the restoration of the vectors  $\bar{L}_s^q$  are used the functions for inverse transform of the components  $\hat{L}_{1s} = \psi_1^{-1}(L_{1s}^q)$ ,  $\hat{L}_{2s} = \psi_2^{-1}(L_{2s}^q)$ ,  $\hat{L}_{3s} = \psi_3^{-1}(L_{3s}^q)$  and in result are obtained the decoded vectors  $\hat{\bar{L}}_s = [\hat{L}_{1s}, \hat{L}_{2s}, \hat{L}_{3s}]^t$ . Using the inverse AKLT, the vectors  $\hat{\bar{L}}_s$  are transformed into vectors  $\hat{\bar{C}}_s = [\hat{C}_{1s}, \hat{C}_{2s}, \hat{C}_{3s}]^t$ :

$$\begin{bmatrix} \hat{C}_{1s} \\ \hat{C}_{2s} \\ \hat{C}_{3s} \end{bmatrix} = \begin{bmatrix} \Phi_{11} & \Phi_{12} & \Phi_{13} \\ \Phi_{21} & \Phi_{22} & \Phi_{23} \\ \Phi_{31} & \Phi_{32} & \Phi_{33} \end{bmatrix} \begin{bmatrix} \hat{L}_{1s} \\ \hat{L}_{2s} \\ \hat{L}_{3s} \end{bmatrix} + \begin{bmatrix} \hat{\bar{C}}_1 \\ \hat{\bar{C}}_2 \\ \hat{\bar{C}}_3 \end{bmatrix} \text{ for } s = 1, 2, \dots, S. \quad (17)$$

Here the matrix of the inverse APCA is:

$$\begin{bmatrix} \Phi_{11} & \Phi_{12} & \Phi_{13} \\ \Phi_{21} & \Phi_{22} & \Phi_{23} \\ \Phi_{31} & \Phi_{32} & \Phi_{33} \end{bmatrix} = [\Phi]^{-1} = [\Phi]^t = [\bar{\Phi}_1, \bar{\Phi}_2, \bar{\Phi}_3]. \quad (18)$$

For the restoration of vectors  $\bar{C}_s = [\hat{C}_{1s}, \hat{C}_{2s}, \hat{C}_{3s}]^t$  through inverse AKLT are needed not only the vectors  $\bar{L}_s = [\hat{L}_{1s}, \hat{L}_{2s}, \hat{L}_{3s}]^t$ , but also the elements  $\Phi_{ij}$  of the matrix  $[\Phi]$ , and the values of  $\bar{C}_1, \bar{C}_2, \bar{C}_3$  as well. The total number of these elements could be reduced representing the matrix  $[\Phi]$  as the product of matrices  $[\Phi_1(\alpha)], [\Phi_2(\beta)], [\Phi_3(\gamma)]$ , and rotation around coordinate axes for each transformed vector in Euler angles  $\alpha, \beta$  and  $\gamma$  correspondingly:

$$[\Phi] = \begin{bmatrix} \Phi_{11} & \Phi_{21} & \Phi_{31} \\ \Phi_{12} & \Phi_{22} & \Phi_{32} \\ \Phi_{13} & \Phi_{23} & \Phi_{33} \end{bmatrix} = [\Phi_1(\alpha)][\Phi_2(\beta)][\Phi_3(\gamma)] = [\Phi(\alpha, \beta, \gamma)], \quad (19)$$

where

$$[\Phi_1(\alpha)] = \begin{bmatrix} \cos\alpha & -\sin\alpha & 0 \\ \sin\alpha & \cos\alpha & 0 \\ 0 & 0 & 1 \end{bmatrix}; [\Phi_2(\beta)] = \begin{bmatrix} \cos\beta & 0 & -\sin\beta \\ 0 & 1 & 0 \\ \sin\beta & 0 & \cos\beta \end{bmatrix}; \quad (20)$$

$$[\Phi_3(\gamma)] = \begin{bmatrix} \cos\gamma & -\sin\gamma & 0 \\ \sin\gamma & \cos\gamma & 0 \\ 0 & 0 & 1 \end{bmatrix}$$

In this case the elements of the matrix  $[\Phi]$  are represented by the relations:

$$\begin{aligned} \Phi_{11} &= \cos\alpha \cos\beta \cos\gamma - \sin\alpha \sin\gamma; \\ \Phi_{21} &= -(\cos\alpha \cos\beta \sin\gamma + \sin\alpha \cos\gamma); \Phi_{31} = -\cos\alpha \sin\beta; \\ \Phi_{12} &= \sin\alpha \cos\beta \cos\gamma + \cos\alpha \sin\gamma; \Phi_{22} = -\sin\alpha \cos\beta \sin\gamma + \cos\alpha \cos\gamma; \\ \Phi_{32} &= -\sin\alpha \sin\beta; \Phi_{13} = \sin\beta \cos\gamma; \Phi_{23} = -\sin\beta \sin\gamma; \Phi_{33} = \cos\beta. \end{aligned} \quad (21)$$

The matrix of the inverse AKLT is defined by the relation:

$$[\Phi]^{-1} = [\Phi_3(-\gamma)][\Phi_2(-\beta)][\Phi_1(-\alpha)] \quad (22)$$

Then, for the calculation of the elements of the inverse matrix  $[\Phi]^{-1}$  is enough to know the values of the 3 rotation angles  $\alpha, \beta$  and  $\gamma$ , defined by the relations:

$$\alpha = -\arcsin\left(\frac{\Phi_{32}}{\sqrt{1-\Phi_{33}^2}}\right); \beta = \arccos(\Phi_{33}); \gamma = \arccos\left(\frac{\Phi_{13}}{\sqrt{1-\Phi_{33}^2}}\right). \quad (23)$$

In result, the number of the needed values for the calculation of the matrix  $[\Phi]^{-1}$  is reduced from 9 down to 3, i.e. 3 times reduction. The elements  $L_{1s}, L_{2s}, L_{3s}$  for

$s=1,2,\dots,S$  comprise the pixels of the first, second and third eigen image in the subgroup of medical images  $C_{1s}, C_{2s}, C_{3s}$ .

#### 4 Experimental results

On the basis of the 2-levels HAKLT algorithm, shown on Fig. 1, were done experiments with sequences of CT images of size  $512 \times 512$  pixels, 8 bpp. The sequence was divided into groups (Set 1,...,Set R), each containing 9 consecutive CT images. As an example, on Fig. 3 is shown one of the groups - Set 3, which contains CT Image 1,..., Image 9.

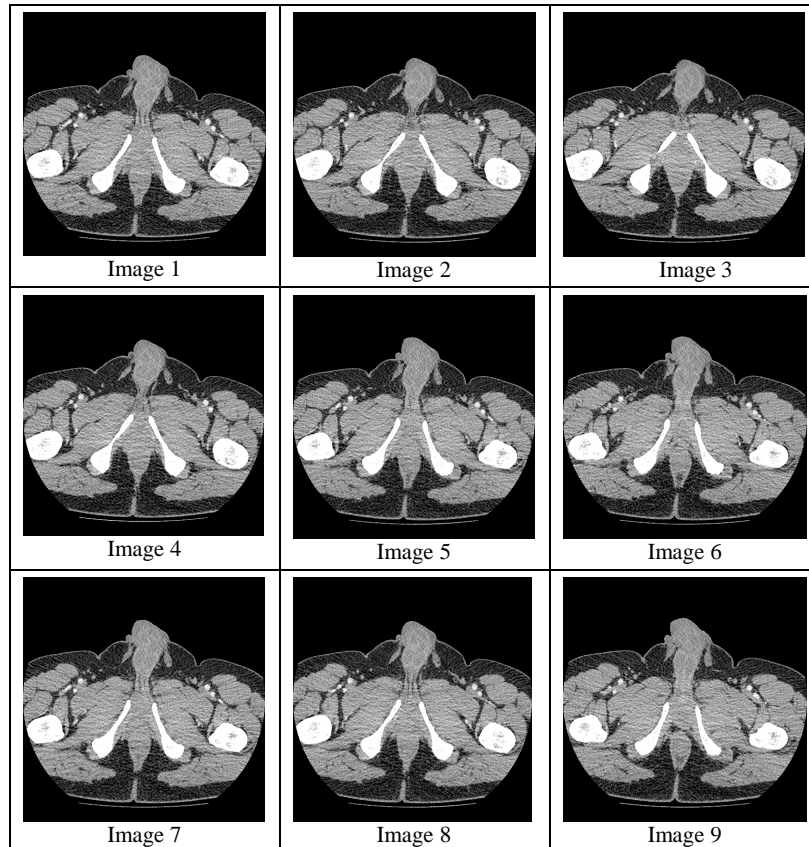


**Fig. 3.** Group of 9 consecutive CT images in Set 3.

On Fig. 4 are shown the corresponding eigen images, obtained in result of applying the 2-levels HAKLT algorithm on the group of images (Set 3).

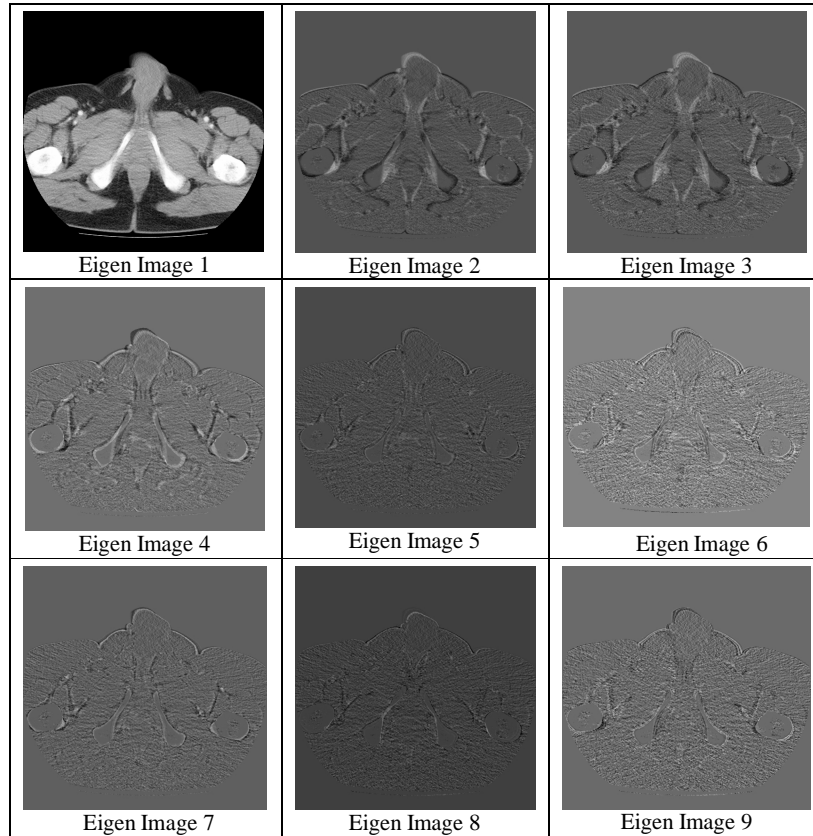


**Fig. 4.** Eigen images, obtained for Set 3 after performing 2-levels HAKLT.

As it could be seen from the results on Fig. 4, on the first eigen image is concentrated the main part of the energy of all 9 images, and the energy of each next eigen image decreases quickly. This conclusion is confirmed by the data given in Table 2, where is given the power distribution of pixels of eigen images from Set 3 after first and second level of HAKLT, before and after their rearrangement in correspondence to Fig. 1. In Table 1 is given the power distribution of all eigen images in Set 3 before and after each operation and the relative mean power distribution. On the basis of data given in Table 1 are build the corresponding graphics, representing the power distribution of all 9 eigen images, shown correspondingly on Figs. 5 - 7.

**Table 1.** Power distribution of all eigen images in Set 3 before and after each operation and relative mean power distribution.

Name	Level 1 (not arranged)	Level 1 (arranged)	Level 2 (not arranged)	Level 2 (arranged)	Relative mean
Eigen Im. 1	18170	18170	53041	53041	219
Eigen Im. 2	715	18056	686	1100	5
Eigen Im. 3	341	18029	316	686	3
Eigen Im. 4	18056	715	1100	710	3
Eigen Im. 5	748	389	710	316	1
Eigen Im. 6	389	694	305	305	1
Eigen Im. 7	18029	341	523	523	2
Eigen Im. 8	694	389	326	326	1
Eigen Im. 9	394	394	242	242	1

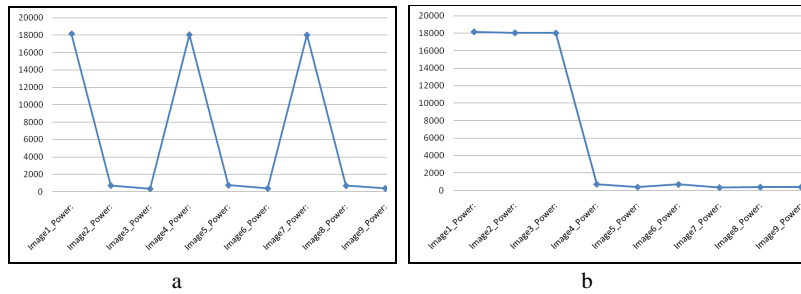


**Fig. 5.** Power distribution for Set 3, level 1: a - not arranged, b - arranged.

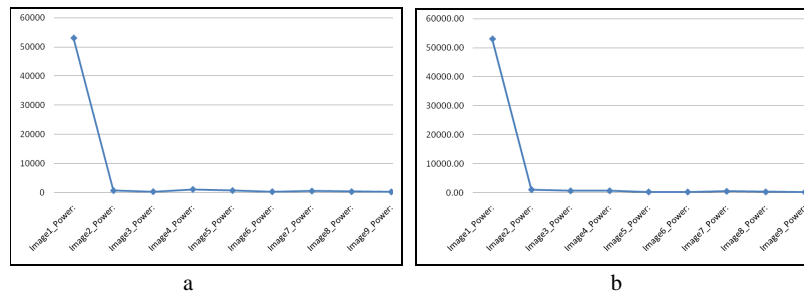


**Fig. 6.** Power distribution for Set 3, level 2: a - not arranged, b - arranged.

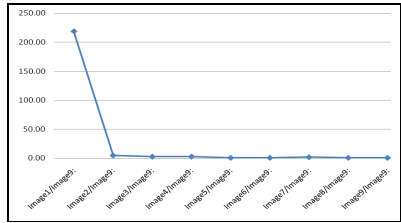
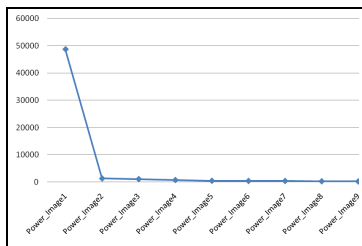


**Fig. 7.** Relative mean power distribution for Set 3, level 2 (arranged)

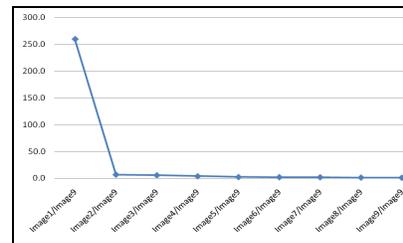
In Table 2 are given the mean and relative mean power distribution of pixels of all 9 eigen images in Set 1,..., Set 7 (R=7), and on Fig. 8 a, b - their corresponding graphic distributions. The data in the last column of Table 2 show, that in the first 3 eigen images are concentrated 95,7 % of the total mean power of all 9 images in GMI.

**Table 2.** Power Distribution, Mean Power Distribution, Relative Mean Power Distribution and Relative Mean % of Power Distribution for all eigen images in Set 1,..., Set 7.

Name	Set 1	Set 2	Set 3	Set 4	Set 5	Set 6	Set 7	Mean	Relative mean	Relative mean %
Eigen Im.1	49992	49749	53041	53547	53774	43272	37701	48725	259.6	91.4
Eigen Im.2	949	811	1100	875	2331	1770	1094	1276	6.8	93.8
Eigen Im.3	683	2325	686	1062	625	834	1144	1051	5.6	95.7
Eigen Im.4	808	710	710	512	460	811	950	709	3.8	97.1
Eigen Im.5	522	566	316	425	300	442	364	419	2.2	97.8
Eigen Im.6	350	529	305	306	317	402	435	378	2.0	98.6
Eigen Im.7	206	222	523	317	554	306	430	365	1.9	99.2
Eigen Im.8	172	198	326	261	312	251	218	248	1.3	99.6
Eigen Im.9	130	171	242	173	254	167	177	188	1.0	100.0



a.



b.

**Fig. 8.** a. Mean Power Distribution; b. Relative Mean Power Distribution for all sets of eigen images

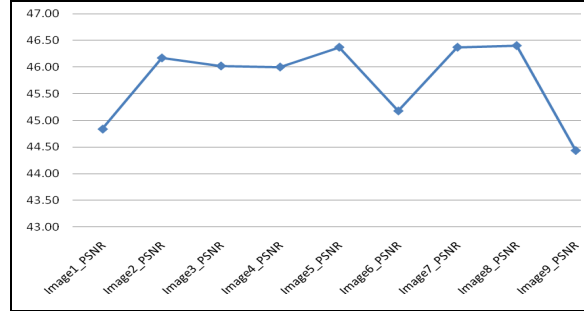


**Fig. 9.** Quality evaluation (through PSNR in dB) of the restored images from Set 3 after Inverse 2-level HAKLT on the eigen images from Fig. 4.

From Fig. 8 b follows that the mean power of the first eigen image for all sets is more than 250 times larger than that of each of the next 8 eigen images.

The values for pixels of the eigen images, obtained in result of the direct 2-level HAKLT, were calculated with full accuracy, and after corresponding rounding could be transformed into 8-bit numbers. Then, if on the 8 bpp eigen images is applied the inverse 2-level HAKLT, the quality of corresponding restored images in GMI, evaluated by their peak signal-to-noise ratio (PSNR), is  $\geq 45$  dB. This was confirmed by the results from Fig. 9, obtained for the eigen images in Set 3 of Fig. 4 after inverse HAKLT in correspondence with the algorithm, shown on Fig.1. Hence, the sequence of 9 images could be restored with retained visual quality. This result illustrates the ability for efficient compression of a sequence of CT images, when HAKLT is used.

The experimental results were obtained with the software implementation of HAKLT, in Visual C.

## 5 Evaluation of the computational complexity

The computational complexity of the 2-level HAKLT algorithm, based on  $3 \times 3$  matrices will be compared with that of the KLT algorithm with a matrix of size  $9 \times 9$ , because 2-level HAKLT is equivalent of the KLT for 9-component vector. For this, both algorithms are compared in respect to the performed number of operations  $S$  (additions and multiplications) [25] needed for the calculation of the following components:

- covariance matrices  $[K_C]$  – in total 6 for the first algorithm, each of size  $3 \times 3$ , and one matrix  $[K_C]$  of size  $9 \times 9$  – for the second algorithm;
- eigen values and eigen vectors of the corresponding matrices  $[K_C]$ ;
- eigen images of each GMI, obtained using both algorithms.

On the basis of the computational complexity analysis given in [24] for AKLT with matrix of size  $3 \times 3$  and for KLT with a matrix of size  $N \times N$  follows, that for the 2-level HAKLT with  $3 \times 3$  matrices and for the KLT with a  $9 \times 9$  matrix we have:

- The number of operations needed for the calculation of all elements  $k_{ij}$  for all 6 matrices  $[K_C]$  of size  $3 \times 3$  (for the 2-level HAKLT) and for one matrix  $[K_C]$  of size  $9 \times 9$  (for the KLT) is:

$$S_k(N) \Big|_{N=3} = 3N(N+1)[N(N-1)+2(N+2)] = 576. \quad (24)$$

$$S_k(N) \Big|_{N=9} = (1/2)N(N+1)[N(N-1)+2(N+2)] = 4230. \quad (25)$$

- The number of operations needed for the calculation of the eigenvalues of matrices  $[K_C]$  for the 2-level HAKLT and of the  $[K_C]$  matrix for KLT, when the QR decomposition and the Householder transform of  $(N-1)$  steps [24] were used, is:

$$S_{val}(N) \Big|_{N=3} = 282. \quad (26)$$

$$S_{val}(N) \Big|_{N=9} = (N-1)\left(\frac{4}{3}N^2 + \frac{17}{6}N + 7\right) = 1124. \quad (27)$$

- The number of operations needed for the calculation of the eigen vectors of matrices  $[K_C]$  for the 2-level HAKLT and for the matrix  $[K_C]$  of KLT, in case that iterative algorithm with 4 iterations is used, is correspondingly:

$$S_{vec}(N) \Big|_{N=3} = 275. \quad (28)$$

$$S_{vec}(N) \Big|_{N=9} = N[2N(4N+5)-1] = 6633. \quad (29)$$

- The number of operations needed for the calculation of a group of 9 eigen images (each of  $P$  pixels), obtained in result of the direct 2-level HAKLT and of KLT for zero mean vectors, is correspondingly:

$$S_{HAKLT}(N) \Big|_{N=3} = 6PN(2N-1) = 90P. \quad (30)$$

$$S_{KLT}(N) \Big|_{N=9} = PN(2N-1) = 153P. \quad (31)$$

Then the total number of operations  $SS$  for the 2-level HAKLT and for KLT is correspondingly:

$$\begin{aligned} SS_1(3) &= [S_k(3) + S_{val}(3) + S_{vec}(3) + S_{HAKLT}(3)] = \\ &= 576 + 282 + 275 + 90P = 1133 + 90P, \end{aligned} \quad (32)$$

$$\begin{aligned} SS_2(9) &= [S_k(9) + S_{val}(9) + S_{vec}(9) + S_{KLT}(9)] = \\ &= 4239 + 1124 + 6633 + 153P = 11996 + 153P. \end{aligned} \quad (33)$$

The reduction of the total number of operations needed for the 2-level HAKLT, compared to that of the KLT could be evaluated using the coefficient  $\eta$ :

$$\eta(P) = \frac{SS_2(9)}{SS_1(3)} = \frac{11996 + 153P}{1133 + 90P}. \quad (34)$$

For example, for  $P=100$   $\eta(100)=2.96$ ; for  $P=1000$  correspondingly  $\eta(1000)=1.81$  and  $\eta(\infty)\rightarrow 1.7$ . Hence,  $SS_1(P)$  is at least 1.7 times smaller than  $SS_2(P)$  for each value of  $P$  (in average, about 2 times).

## 6 Conclusions

The basic qualities of the offered HAKLT for processing a group of sequential medical images are:

1. Lower computational complexity than KLT for the whole GMI, due to the lower complexity of AKLT compared to the case, for which for the calculation of the KLT matrix are used numerical methods [15, 16];
2. Ability for efficient lossy compression of GMI with retained visual quality of the restored images and for lossless compression also;
3. Ability for minimization of features space in the regions of interest in a group of medical images, which contain searched objects of various kinds;
4. There is also a possibility for further development of the HAKLT algorithm, through: use of Integer KLT for lossless coding of medical images by analogy approach with [23]; compression of video sequences from stationary TV camera; sequences of multispectral and multi-view images, etc.

## Acknowledgement

This paper was supported by the Joint Research Project Bulgaria-Romania (2010-2012): "Electronic Health Records for the Next Generation Medical Decision Support in Romanian and Bulgarian National Healthcare Systems" DNTS 02/19 and the Research Project No 122PD0061-07, supported by RD sector of TU-Sofia.

## References

1. Gonzales, R., Woods, R.: Digital Image Processing, 3<sup>rd</sup> Ed., Prentice Hall (2008)
2. Rangayyan, R.: Biomedical Image Analysis, CRC Press, Boca Raton (2005)
3. Dougherty, G.: Digital Image Processing for Medical Applications, Cambridge University Press (2009)
4. Graham, R., Perris, R., Scarsbrook, A.: DICOM demystified: A review of digital file formats and their use in radiological practice. Clinical Radiology, 60: 1133-1140 (2005)
5. Wu, Y.: Medical image compression by sampling DCT coefficients, IEEE Trans. on Information Technology in Biomedicine, 6 (1): 86-94 (2002)
6. Ramesh, S., Shanmugam, D.: Medical image compression using wavelet decomposition for prediction method, International Journal of Computer Science and Information Security (IJCSIS) 7(1): 262-265 (2010)
7. Lalitha, Y., Latte, M.: Image compression of MRI image using planar coding. Intern. J. of Advanced Computer Science and Applications (IJACSA), 2 (7): 23-33 (2011)

8. Roos, P., Viergever, M.: Reversible interframe compression of medical images: a comparison of decorrelation methods, *IEEE Trans. Medical Imaging*, 10 (4): 538-547 (1991)
9. Reed, T. (ed.). *Digital Image Sequence Processing, Compression, and Analysis*, CRC Press (2004)
10. Szilágyi, S., Szilágyi, L., Benyó, Z.: Echocardiographic Image Sequence Compression Based on Spatial Active Appearance Model, *Progress in Pattern Recognition, Image Analysis and Applications*, LN in Computer Science, 4756: 841-850 (2007)
11. Miaou, S., Ke, F., Chen, S.: A Lossless Compression Method for Medical Image Sequences Using JPEG-LS and Interframe Coding, *IEEE Trans. on Inform. Techn. in Biomedicine*, 13 (5): 818-821 (2009)
12. Bitaa, I., Barretb, M., Phamc, D.: On Optimal Transforms in Lossy Compression of Multicomponent Images with JPEG2000, *SP*, 90(3): 759-773 (2010)
13. Thirumalai, V.: *Distributed Compressed Representation of Correlated Image Sets*, Thesis No 5264, Lausanne, EPFL (2012)
14. Jain, A.: A fast Karhunen-Loeve transform for a class of random processes, *IEEE Trans. Commun. Vol. COM-24*: 1023-1029 (1976)
15. Dony, R.: Karhunen-Loeve Transform, Chapter 1 in *The transform and data compression handbook* (Eds. K. Rao and P. Yip), Boca Raton, CRC Press (2001)
16. Jolliffe, I.: *Principal Component Analysis*, 2nd ed., Springer-Verlag, NY (2002)
17. Ujwala, P., Uma, M.: Image Fusion using Hierarchical PCA, *Intern. Conf. on Image Information Processing (ICIIP)*: 1-6 (2011)
18. Hanafi, M., Kohler, A., Qannari, E.: Shedding new light on Hierarchical Principal Component Analysis, *J. of Chemometrics*, 24 (11-12): 703-709 (2010)
19. Langs, G., Bischof, H., Kropatsch, W.: Hierarchical Top Down Enhancement of Robust PCA, T. Caelli et al. (Eds.), *SSPR&SPR, LNCS 2396*, Springer: 234-243 (2002)
20. Grasedyck, L.: Hierarchical Singular Value Decomposition of Tensors, Preprint 20, AG Numerik/Optimierung, Philipps-Universität Marburg: 1-29 (2009)
21. Diamantaras, K., Kung, S.: *Principal Component Neural Networks: Theory and Applications*, John Wiley & Sons, NY (1996)
22. Solo, V., Kong, X.: Performance analysis of adaptive eigen analysis algorithms, *IEEE Trans. Signal Processing*, 46 (3): 636-645 (1998)
23. Hao, P., Shi, Q.: Reversible Integer KLT for Progressive-to-Lossless Compression of Multiple Component Images. *IEEE ICIP*, Barcelona, Spain (2003)
24. Kountchev, R., Kountcheva, R.: Image Color Space Transform with Enhanced KLT, In: *New Advances in Intelligent Decision Technologies*, Eds. K. Nakamatsu, G. Wren, L. Jain, R. Howlett. Springer: 171-182 (2009)
25. Arora, S., Barak, B.: *Computational Complexity: A Modern Approach*, Cambridge University Press (2009)